Quantum-statistical property of optical diode based on cavity QED

Haozhen Li,[1,2] Jingping Xu,[1,*] Da-Wei Wang,[2] Xiuwen Xia,[3] Yaping Yang,[1,†] and Shiyao Zhu[4]

[1]*Key Laboratory of Advanced Micro-Structured Materials of Ministry of Education, School of Physics Science and Engineering, Tongji University, Shanghai 200092, China*

[2]*Institute for Quantum Science and Engineering, Texas A&M University, College Station, Texas 77845, USA*

[3]*School of Mathematics and Physics, Jinggangshan University, Ji'an, Jiangxi 343009, China*

[4]*Department of Physics, Zhejiang University, Hangzhou 310027, China*

(Received 24 March 2017; published 17 July 2017)

An optical diode made of an asymmetric cavity containing a two-level atom is investigated. We focus on the quantum-statistical property of the transmitted field with nonclassical light input. Both coherent and squeezed light inputs have been considered. The results show that the transmitted contrast of such optical diode is independent of the statistical properties of the incident light but is only sensitive to its intensity. On the other hand, the quantum-statistical property, i.e., the squeezing, of the transmitted field strongly depends on the statistical properties and directions of the incident light. For squeezed light input, the degree of the squeezing of the transmitted field can be remarkably enhanced. Moreover, the squeezing of the amplitude quadrature of the incident light can be transferred to the phase quadrature due to the coupling of the light and the atom.

DOI: 10.1103/PhysRevA.96.013832

I. INTRODUCTION

Cavity quantum electrodynamics (QED), where atoms are coupled with a quantum field in a cavity, gives rise to many fundamental, interesting effects such as vacuum Rabi splitting [1,2], nonclassical light generation [3,4], and optical nonlinearity [5,6]. Most of these effects have been verified by experiments [7–12]. Besides, cavity QED enables an increasing number of applications to quantum states transfer [13,14], photon absorption [15,16], all-optical transistor [17,18], optical bistability [19–23], optical nonreciprocity [24–26], and so on. Optical nonreciprocity is the essence of the optical diode [27], which is a core element in all-optical signal processing systems. There were many theoretical and experimental proposals based on photonic crystal [28,29], one-dimensional waveguides [30,31] and other systems [32–34] to achieve optical diode. However, most of them are suitable only to a classical field input. Inspired by the progress in quantum information, the diode operation under nonclassical light input deserves investigation. Although there were several papers considering optical diode at a few- and even single-photon level [35–37], the behavior of the optical diode with the squeezed or the coherent light input as well as the quantum-statistical properties of the corresponding transmitted light are rarely considered.

Quantum-statistical properties of the light emitted by the atom in an optical cavity have been studied by many authors [38–46], including bunching and antibunching [42,43], the spectrum of the second-order correlation [44], photon blocking [45], and squeezing [46]. In particular, the squeezing is regarded as one of the most peculiar nonclassical phenomena in quantum systems. It plays a crucial role in the precision measurements and the noiseless communications. A variety of schemes have been presented to generate the squeezed states to date [47–51]. One of the proposals is the cavity system containing an optical nonlinear medium, i.e., a degenerate-parametric amplifier [47,51]. The others include basic cavity QED systems [52,53], semiconductor systems [54], and cavity optomechanics systems [55–58]. The physics behind them is mainly related to the nonlinear optical process. Thus one way to improve the degree of squeezing is to enhance the nonlinearity of the system.

In this paper, we continue the study of the optical diode based on cavity QED reported in Ref. [23], and focus on the quantum-statistical property of such optical diode with the coherent and the squeezed light input. It is found that the transmission contrast of the optical diode is independent of the statistical properties of the incident light but sensitive to the intensity. Furthermore, we reveal that the quantum-statistical property of the transmitted field can be manipulated by varying the cavity-loss rate, the direction, the intensity, and the quantum-statistical properties of the incident light.

This paper is organized as follows. In Sec. II, we introduce the cavity QED system, in which an asymmetric cavity contains a two-level atom, and the basic theory to describe the input-output relationship as well as the quantum-statistical property of the system. In Sec. III, we analyze the optical diode effect with the coherent and the squeezed light input. In Sec. IV, we explore the corresponding quantum-statistical property of the transmitted field. Finally, conclusions are drawn in Sec. V.

II. MODEL AND BASIC THEORY

We consider an atom-asymmetric cavity coupling system in the reservoirs, as shown in Fig. 1. There is a two-level atom with transition frequency ω_0 embedded at the center of the single-mode cavity with frequency ω_c. The cavity mode couples to the outside continuum modes with coupling constants g_1 and g_2, respectively. The difference between g_1 and g_2 originates from the asymmetric cavity with different reflective walls M_1 and M_2. The Hamiltonian of the whole system under a rotating-wave approximation is given as

*xx_jj_pp@hotmail.com

†yang_yaping@tongji.edu.cn

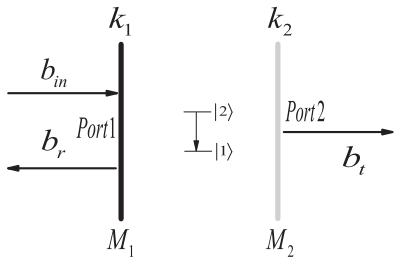

FIG. 1. Scheme of the atom-cavity coupling system.

follows:

$$H = H_S + H_R + H_I, \tag{1}$$

where

$$H_S = \hbar\omega_0 S_z + \hbar\omega_c a^\dagger a + \hbar\Omega(a^\dagger S_- + S_+ a) \tag{2}$$

is the Hamiltonian of the atom-cavity coupling system. The first two terms represent the Hamiltonian of the atom and the cavity mode, respectively. The last term represents the interaction between the cavity mode and the atom with a coupling coefficient Ω. a ($a^\dagger$) is the annihilation (creation) operator of the cavity mode. $S_- = |1\rangle\langle 2|$ and $S_z = (|2\rangle\langle 2| - |1\rangle\langle 1|)/2$ are atomic operators.

$$H_R = \hbar\sum_k \omega_k b_k^\dagger b_k + \hbar\sum_l \omega_l c_l^\dagger c_l \tag{3}$$

is the Hamiltonian of the reservoirs. Here b_k and c_l are the annihilation operators of the modes for port 1 and port 2, respectively; ω_k and ω_l are their corresponding frequencies.

$$H_I = \hbar\sum_k g_1(b_k^\dagger a + a^\dagger b_k) + \hbar\sum_l g_2(c_l^\dagger a + a^\dagger c_l) \tag{4}$$

is the interaction Hamiltonian between the cavity mode and the reservoir modes. When there is an external field input from the left side to the right side (from M_1 to M_2), we call it the forward incidence, as shown in Fig. 1. On the contrary, the backward incidence refers to the light input from the right side (from M_2 to M_1). As the atom is located at the center of the cavity, the backward input case is equivalent to the forward case by just interchanging the values of g_1 and g_2.

Here we consider a monochromatic external field input from the left side, i.e., the forward input case. According to the Heisenberg equations $\partial\hat{O}/\partial t = [\hat{O},\hat{H}]/i\hbar$, and considering the atomic dissipation, the equations of relevant operators in the frame rotating at the input frequency ω are obtained as [5]

$$\dot{S}_- = -(i\Delta + \gamma_{\rm at}/2)S_- + 2i\Omega S_z a, \tag{5}$$

$$\dot{S}_z = -i\Omega S_+ a + i\Omega a^\dagger S_- - \gamma_{\rm at}(S_z + 1/2), \tag{6}$$

$$\dot{a} = -i\delta a - i\Omega S_- - \kappa a - i\sqrt{\kappa_1}b_{\rm in}, \tag{7}$$

$$b_t = -i\sqrt{\kappa_2}a. \tag{8}$$

Here $\gamma_{\rm at}$ is the dissipation rate of the atom, $\Delta = \omega_0 - \omega$ ($\delta = \omega_c - \omega$) is the detuning between the atom (cavity) and the input field. $\kappa_1 = |g_1|^2\tau_k$ and $\kappa_2 = |g_2|^2\tau_l$ are denoted as the cavity-loss rates from port 1 and port 2, respectively, where τ_j is defined by $\sum_j e^{-i\omega_j t} = \delta(t)\tau_j$, ($j = k,l$). $\kappa = (\kappa_1 + \kappa_2)/2$ represents the average cavity-loss rate. The incident and transmitted operators are introduced as [5,59]

$$\begin{aligned} b_{\rm in}(t) &= \frac{1}{\sqrt{\tau_k}}\sum_k b_k(t_0)e^{-i\omega_k(t-t_0)}, \quad t > t_0, \\ b_t(t) &= \frac{1}{\sqrt{\tau_l}}\sum_l c_l(t_0')e^{-i\omega_l(t-t'_0)}, \quad t < t'_0. \end{aligned} \tag{9}$$

The operator equations, Eqs. (5)–(8), are the starting point of our analysis. Generally, the ratio $C = 4\Omega^2/\kappa\gamma_{\rm at}$ can measure all aspects of the atom-cavity interaction, and is defined as the single atom-cavity cooperativity parameter (also called the Purcell factor). $C > 1$ refers to the strong coupling, while $C \ll 1$ refers to the weak coupling. In this work, we fix the average cavity-loss rate $\kappa = 500\gamma_{\rm at}$, and just change the value of κ_1 to achieve the asymmetric cavity. Therefore the systems work at the same coupling regime with constant C. In addition we set $\Delta = \delta = 0$ to enhance the coupling among atom, cavity mode, and input field. In the next section we will discuss the input-output relations with different input fields: the coherent field and the squeezed field.

III. OPTICAL DIODE EFFECT WITH THE COHERENT AND THE SQUEEZED FIELD INPUT

For the coherent input field, it leads to the following expectation values as

$$\begin{aligned} \langle b_{\rm in}\rangle &= |\alpha|e^{i\phi/2}, \\ \langle b_{\rm in}^\dagger b_{\rm in}\rangle &= |\alpha|^2, \\ \langle b_{\rm in} b_{\rm in}\rangle &= |\alpha|^2 e^{i\phi}. \end{aligned} \tag{10}$$

Here α is a complex number with angle ϕ. It is the eigenvalue of the operator $b_{\rm in}$ whose eigenstate is the coherent state. $|\alpha|^2$ is the average photon number. For the squeezed input field, the corresponding expectation values are

$$\begin{aligned} \langle b_{\rm in}\rangle &= \langle b_{\rm in}^\dagger\rangle = 0, \\ \langle b_{\rm in}^\dagger b_{\rm in}\rangle &= \sinh^2 r, \\ \langle b_{\rm in} b_{\rm in}\rangle &= -\cosh r e^{i\eta}\sinh r. \end{aligned} \tag{11}$$

Here r is the squeezing factor of the incident light; η is the squeezed angle. It is clear that the average intensity of the squeezed input field is $\sinh^2 r$.

In this section, we analyze the optical diode effect with the coherent or the squeezed light input in the steady state. Here $n_t = b_t^\dagger b_t$ scales like a transmitted photon number per unit of time which represents the output power, and $n_c = a^\dagger a$ is the photon numbers in the cavity. The relations between n_t and n_c can be obtained through Eq. (8) as

$$n_t = \kappa_2 n_c, \tag{12}$$

and then the steady atomic dipole moment S_- can be expressed from Eq. (5) as

$$S_- = 4i\Omega S_z a\big/\gamma_{\rm at}. \tag{13}$$

Inserting Eqs. (12) and (13) into Eq. (6), we obtain the steady atomic population S_z as

$$S_z = -\frac{1}{2}\frac{1}{1+x}, \tag{14}$$

where $x = n_t/P_{ct}$ is the saturation parameter, in which $P_{ct} = \kappa_2\gamma_{at}^2/8\Omega^2$ is the critical power of n_t to reach $S_z = -1/4$. Inserting Eq. (13) into Eq. (7), we can relate the cavity field operator a to the input field operator b_{in} as

$$\left(\kappa - \frac{4\Omega^2 S_z}{\gamma_{at}}\right)a = -i\sqrt{\kappa_1}b_{in}. \tag{15}$$

After multiplying their conjugation operator, the relation between $\langle n_{in}\rangle$ and $\langle n_t\rangle$ takes the form as

$$\langle n_{in}\rangle = \frac{\langle n_t\rangle}{\kappa_1\kappa_2}\left[\frac{2\Omega^2}{\gamma_{at}(1+x)} + \kappa\right]^2, \tag{16}$$

where $n_{in} = b_{in}^\dagger b_{in}$ scales like the input photon numbers and represents the input power. Equation (16) indicates that the transmitted power $\langle n_t\rangle$ directly relates to the input power $\langle n_{in}\rangle$, but independent of the statistical properties of the input field ($\langle b_{in}\rangle$, $\langle b_{in}b_{in}\rangle$). For simplification, we just use n_i to represent $\langle n_i\rangle (i = in,t)$ in the following. Here, we restricted ourselves to the Purcell regime ($C = 4\Omega^2/\kappa\gamma_{at} \gg 1$). Furthermore, the coupling coefficient Ω is larger than the dissipation rates of the atom, but is much less than the cavity-loss rates; i.e., $\gamma_{at} < \Omega \ll \kappa$. We set $\Omega = 50\gamma_{at}$ and $\kappa = 500\gamma_{at}$ as the common parameters to perform the analysis. In the following, the input-output relations of the system with coherent light input have been discussed in detail.

In Fig. 2, we plot the input-output relations for both the symmetric ($\kappa_1 = \kappa_2 = \kappa$) and the asymmetric ($\kappa_1 \neq \kappa_2$) cavity under the coherent light input. It is found that the transmitted photon numbers display a counterclockwise hysteresis in all cases, which means the appearance of the optical bistable states. There are two threshold values to identify the bistable regime. When the input power $n_{in} = |\alpha|^2$ is smaller than the lower threshold value, the light is almost blocked; when the input power is larger than the higher threshold value, the light can transmit through the system easily. Moreover, Fig. 2 indicates that the bistable regime can be affected by the asymmetry of the cavity.

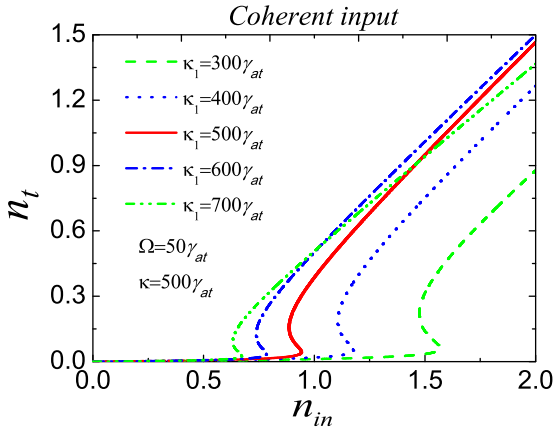

FIG. 2. The output photon number n_t as a function of input power n_{in} with different cavity-loss rate κ_1. The red solid curve represents the symmetric cavity with $\kappa_1 = 500\gamma_{at}$, the green dashed, blue dotted, blue dash-dotted, and green dash-dot-dotted curves correspond to $\kappa_1 = 300\gamma_{at}, 400\gamma_{at}, 600\gamma_{at}$, and $700\gamma_{at}$, respectively. The common parameter is $\kappa = 500\gamma_{at}$.

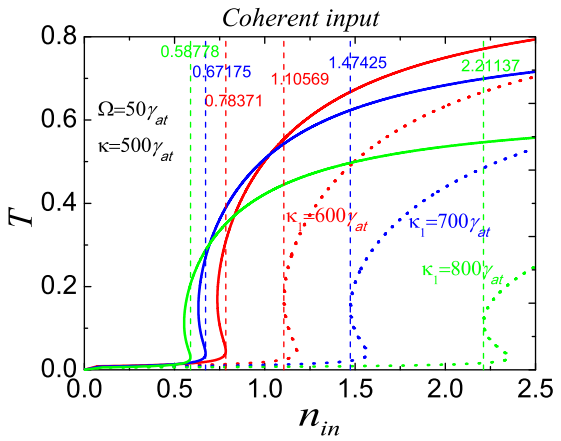

FIG. 3. The transmittivity ($T = n_t/n_{in}$) for both forward and backward incidence as a function of input power n_{in} with different cavity-loss rate κ_1. All the solid (dotted) curves represent the forward (backward) incidence respectively. The red, blue, and green vertical dashed curves correspond to the threshold values of each optimal window with $\kappa_1 = 600\gamma_{at}, 700\gamma_{at}$, and $800\gamma_{at}$, respectively. The common parameter is $\kappa = 500\gamma_{at}$.

When $\kappa_1 > \kappa$, i.e., $\kappa_1 = 600\gamma_{at}$ and $700\gamma_{at}$, the bistable regime shifts to the lower input power (see the blue dash-dotted and green dash-dot-dotted curves). Oppositely, when $\kappa_1 < \kappa$, i.e., $\kappa_1 = 400\gamma_{at}$ and $300\gamma_{at}$, the bistable regime moves to the higher input power (see the blue dotted and green dashed curves).

If we define $\kappa_1 > \kappa$ as the forward incidence, then the cases of $\kappa_1 < \kappa$ are equivalent to the backward incidence. In Fig. 3, we plot the transmissivity ($T = n_t/n_{in}$) for both the forward and the backward incident light as a function of the input power n_{in}. It shows that the bistable regimes of the forward input are separated from those of the backward input due to the asymmetry of the cavity. When the input power falls into the range between these two bistable regimes, the input light can only transmit through the system in the forward direction. For example, in the case of $\kappa_1 = 600\gamma_{at}$, when the input power falls into the regime [0.78,1.11], $T > 0.3$ for the forward incidence, while $T < 0.02$ for the backward incidence (see the red solid and dashed curves in Fig. 3). This means that the separation of the bistable regimes leads to the optical diode effect.

Furthermore, Fig. 3 indicates clearly that the width of the optimal window can be significantly affected by the asymmetry of the cavity, i.e., the difference among the cavity-loss rates ($|\kappa_1 - \kappa_2|$). With the increasing of $|\kappa_1 - \kappa_2|$, the width of the optimal window can be enlarged (see the blue solid, dashed curves and green solid, dashed curves, respectively), and the transmitted contrast for each window will be enhanced accordingly, which will be discussed in the following.

In Fig. 4, we plot the transmitted contrast, $C_T = 10|\log_{10}(T_f/T_b)|$, as a function of the input power with different cavity-loss rate κ_1 within the corresponding optimal

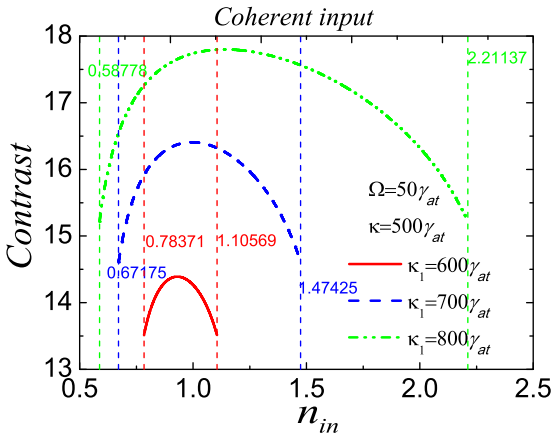

FIG. 4. The transmitted contrast $C_T = 10|\log_{10}(T_f/T_b)|$ as a function of the input power with different cavity-loss rate κ_1.The red, blue, and green vertical dashed curves refer to the threshold values of each optimal window with $\kappa_1 = 600\gamma_{at}, 700\gamma_{at}$, and $800\gamma_{at}$, respectively. The common parameter is $\kappa = 500\gamma_{at}$.

operation power windows. It is found that the optical diode works with a high transmitted contrast and low input power within each optimal input window. The transmitted contrast increases to its maximal at first, and then decreases with the input power. Moreover, the transmit contrast is also affected by the cavity-loss rate κ_1. The larger the cavity-loss rate κ_1 is, the wider the optimal input window, and the higher the transmit contrast accordingly.

From the above discussions, it is clear that an optical diode can be realized based on the single atom-asymmetrical cavity coupling system with coherent light input. Actually, the input-output relations with squeezed light input also have been investigated. It is confirmed that the diode effect is regained and the results are the same as the coherent input case, except that the intensity of the squeezed input is expressed by $n_{\rm in} = \sinh^2 r$. Obviously, the behavior of the diode only depends on the average power of the input field, and does not relate to the quantum-statistics character of the input field, which is consistent with the previous works only considering the classical field input [23]. However, the nonlinearity of the system would change the state of field in general, so we will discuss the quantum-statistical character of the transmitted field in Sec. IV.

IV. QUANTUM-STATISTICAL PROPERTIES OF THE OUTPUT FIELD

In this section, we proceed to analyze the squeezing properties of the transmitted field. The cavity field variance can be obtained from Eqs. (5)–(7) by using the notation $\langle A,B\rangle = \langle AB\rangle - \langle A\rangle\langle B\rangle$, read as

$$\langle a,a\rangle = \frac{\kappa_1[2\Omega^2 - \kappa\gamma_{\rm at}(1+x)]}{\kappa^2[2\Omega^2 + \kappa\gamma_{\rm at}(1+x)]}\langle b_{\rm in},b_{\rm in}\rangle + \frac{4\kappa_1\Omega^4}{\kappa^2[2\Omega^2 + \kappa\gamma_{\rm at}(1+x)]^2}\langle b_{\rm in}\rangle^2, \tag{17}$$

$$\langle a^\dagger,a\rangle = -\frac{\kappa_1[2\Omega^2 - \kappa\gamma_{\rm at}(1+x)]}{\kappa^2[2\Omega^2 + \kappa\gamma_{\rm at}(1+x)]}\langle b_{\rm in}^\dagger,b_{\rm in}\rangle - \frac{4\kappa_1\Omega^4}{\kappa^2[2\Omega^2 + \kappa\gamma_{\rm at}(1+x)]^2}\langle b_{\rm in}^\dagger\rangle\langle b_{\rm in}\rangle + \frac{\Omega^2 x}{2\kappa^2(1+x)}. \tag{18}$$

The variance of the transmitted field operator can be obtained by using the input-output relation, Eq. (8), read as [60]

$$\langle b_t,b_t\rangle = -\kappa_2\langle a,a\rangle, \tag{19}$$

$$\langle b_t^\dagger,b_t\rangle = \kappa_2\langle a^\dagger,a\rangle. \tag{20}$$

To measure the squeezing, the output field must be expressed in terms of the quadrature components. For example, the Hermitian operator b_t should be divided into two quadrature components as [60]

$$b_t = e^{i\theta/2}(T_1 + iT_2). \tag{21}$$

These two components T_1 and T_2 satisfy the commutation relation as $[T_1,T_2] = i/2$. $\theta/2$ is the axes rotating angle between T_1 and T_2. Then the variance of these two quadrature components of the transmitted field takes the following forms:

$$\langle :\delta T_1^2: \rangle = -\frac{\kappa_1\kappa_2}{4\kappa^2}\left(\left\{\frac{2\Omega^2 - \kappa\gamma_{\rm at}(1+x)}{2\Omega^2 + \kappa\gamma_{\rm at}(1+x)}\langle b_{\rm in},b_{\rm in}\rangle + \frac{4\Omega^4}{[2\Omega^2 + \kappa\gamma_{\rm at}(1+x)]^2}\langle b_{\rm in}\rangle^2\right\}e^{-i\theta} + {\rm c.c.}\right) - \frac{\kappa_1\kappa_2[2\Omega^2 - \kappa\gamma_{\rm at}(1+x)]}{2\kappa^2[2\Omega^2 + \kappa\gamma_{\rm at}(1+x)]}\langle b_{\rm in}^\dagger,b_{\rm in}\rangle - \frac{2\kappa_1\kappa_2\Omega^4}{\kappa^2[2\Omega^2 + \kappa\gamma_{\rm at}(1+x)]^2}\langle b_{\rm in}^\dagger\rangle\langle b_{\rm in}\rangle + \frac{\kappa_2\Omega^2 x}{4\kappa^2(1+x)}, \tag{22}$$

$$\langle :\delta T_2^2: \rangle = \frac{\kappa_1\kappa_2}{4\kappa^2}\left\{\frac{2\Omega^2 - \kappa\gamma_{\rm at}(1+x)}{2\Omega^2 + \kappa\gamma_{\rm at}(1+x)}\langle b_{\rm in},b_{\rm in}\rangle + \frac{4\Omega^4}{[2\Omega^2 + \kappa\gamma_{\rm at}(1+x)]^2}\langle b_{\rm in}\rangle^2 e^{-i\theta} + {\rm c.c.}\right\} - \frac{\kappa_1\kappa_2[2\Omega^2 - \kappa\gamma_{\rm at}(1+x)]}{2\kappa^2[2\Omega^2 + \kappa\gamma_{\rm at}(1+x)]}\langle b_{\rm in}^\dagger,b_{\rm in}\rangle - \frac{2\kappa_1\kappa_2\Omega^4}{\kappa^2[2\Omega^2 + \kappa\gamma_{\rm at}(1+x)]^2}\langle b_{\rm in}^\dagger\rangle\langle b_{\rm in}\rangle + \frac{\kappa_2\Omega^2 x}{4\kappa^2(1+x)}. \tag{23}$$

The above variances originate from the definition of $\langle :\delta T_i^2: \rangle = \langle T_i,T_i\rangle - \frac{1}{4}$, $i = 1,2$. If $\langle :\delta T_i^2: \rangle$ is negative, the output field exhibits quadrature squeezing. In detail, $\langle :\delta T_1^2: \rangle$ measures the amplitude quadrature squeezing, while $\langle :\delta T_2^2: \rangle$ measures the phase quadrature squeezing. According to the definition of $\langle A,B\rangle = \langle AB\rangle - \langle A\rangle\langle B\rangle$, it is clear from Eqs. (22) and (23) that the squeezing properties of the transmitted field relate to not only the average intensity

$\langle b_{\rm in}^{\dagger} b_{\rm in}\rangle$ but also the statistical properties ($\langle b_{\rm in}\rangle$, $\langle b_{\rm in} b_{\rm in}\rangle$) of the input fields. Besides, the squeezing depends on the system's parameters, i.e., $\gamma_{\rm at}$,Ω,κ,κ_1,κ_2. Because the coherent field has different statistical properties from the squeezed field, shown in Eqs. (10) and (11), the variances of these two quadratures of the transmitted field $\langle{:}\,\delta T_1^2\,{:}\rangle$ and $\langle{:}\,\delta T_2^2\,{:}\rangle$ are much different between the coherent and the squeezed input fields. This is the key point that leads to the remarkably different quantum-statistical properties of the transmitted field in these two cases, which are discussed below.

A. Coherent light input

In this part, we analyze the squeezing properties of the output field with the coherent light input. According to Eqs. (22) and (23) and combining with Eq. (10), the variances of the output field are obtained as follows:

$$\langle{:}\,\delta T_1^2\,{:}\rangle = -\frac{4\kappa_1\kappa_2\Omega^4|\alpha|^2}{\kappa^2[2\Omega^2+\kappa\gamma_{\rm at}(1+x)]^2} + \frac{\kappa_2\Omega^2 x}{4\kappa^2(1+x)}, \tag{24}$$

$$\langle{:}\,\delta T_2^2\,{:}\rangle = \frac{\kappa_2\Omega^2 x}{4\kappa^2(1+x)}. \tag{25}$$

From Eq. (25), it is found that $\langle{:}\,\delta T_2^2\,{:}\rangle$ is always positive; that is, the squeezing disappears in the phase quadrature. Therefore, we only focus on the amplitude quadrature $\langle{:}\,\delta T_1^2\,{:}\rangle$ here. $\langle{:}\,\delta T_1^2\,{:}\rangle$ as a function of the input power $n_{\rm in}=|\alpha|^2$ with different cavity-loss rate κ_1 is shown in Fig. 5(a). It is found that, for the forward incidence, with the increasing of input power $n_{\rm in}$, the squeezing ($\langle{:}\,\delta T_1^2\,{:}\rangle < 0$) increases to maximal at first. Then the squeezing will decrease with further increasing of $n_{\rm in}$, and even disappear ($\langle{:}\,\delta T_1^2\,{:}\rangle \geqslant 0$) when $n_{\rm in}$ is shifted into the optimal input window. This phenomenon relates to the nonlinear saturation of the atom. When the input power is weak, the atom in the cavity cannot be saturated; thus the coupling between the atom and the input light can be enhanced with the increase of the input photons, which leads to the enhancement of the squeezing. By further increasing the input photons, the atom will be saturated gradually; thus the coupling between the atom and the input light becomes weaker, and consequently, the squeezing decreases. When the input photon numbers fall into the optimal input window, the input power is sufficient to saturate the atom; thus the transmitted light will decouple from the atom completely, and as a result, the squeezing disappears [see the solid curves in Fig. 5(a)]. For the backward incidence, the squeezing behaviors are very similar to that of the forward incidence, except that when the input power falls into the optimal input window, it still cannot saturate the atom, so the squeezing remains for the backward input even if the input power is shifted into the optimal input window [see the dashed curves in Fig. 5(a)]. In order to show the effect of the direction of the incident light on the squeezing more clearly, we plot the variance $\langle{:}\,\delta T_1^2\,{:}\rangle$ under each optimal inputting window with $\kappa_1 = 600\gamma_{\rm at}$, $700\gamma_{\rm at}$, and $800\gamma_{\rm at}$ in Fig. 5(b). It turns out that the squeezing ($\langle{:}\,\delta T_1^2\,{:}\rangle < 0$) can only be observed for the backward case while there is no squeezing ($\langle{:}\,\delta T_1^2\,{:}\rangle \geqslant 0$) for the forward incidence.

Furthermore, when the input power is smaller than the lower threshold value of the optimal operation power window (i.e., $n_{\rm in} < 0.78371$ for $\kappa_1 = 600$), the degree of squeezing for the forward incidence is smaller than that for the backward incidence [see the red solid and dashed curves in Fig. 5(a)]. For the forward incidence, the amount of the squeezing decreases with the increase of the cavity-loss rate κ_1 [see the solid blue and green curves in Fig. 5(a)], while for the backward incidence, the squeezing increases [see the dotted blue and green curves in Fig. 5(a)]. It is obvious that the squeezing of the transmitted field for the backward incidence is much more significant than that for the forward case.

B. Squeezed light input

Here we discuss the squeezing effects of the transmitted field with an amplitude quadrature squeezed light input. The variance $\langle{:}\,\delta T_i^2\,{:}\rangle$ of the transmitted field can be obtained from Eqs. (22), (23), and (11) as

$$\langle{:}\,\delta T_1^2\,{:}\rangle = \frac{\kappa_1\kappa_2[2\Omega^2-\kappa\gamma_{\rm at}(1+x)](\cosh r\sinh r-\sinh^2 r)}{2\kappa^2[2\Omega^2+\kappa\gamma_{\rm at}(1+x)]} + \frac{\kappa_2\Omega^2 x}{4\kappa^2(1+x)}, \tag{26}$$

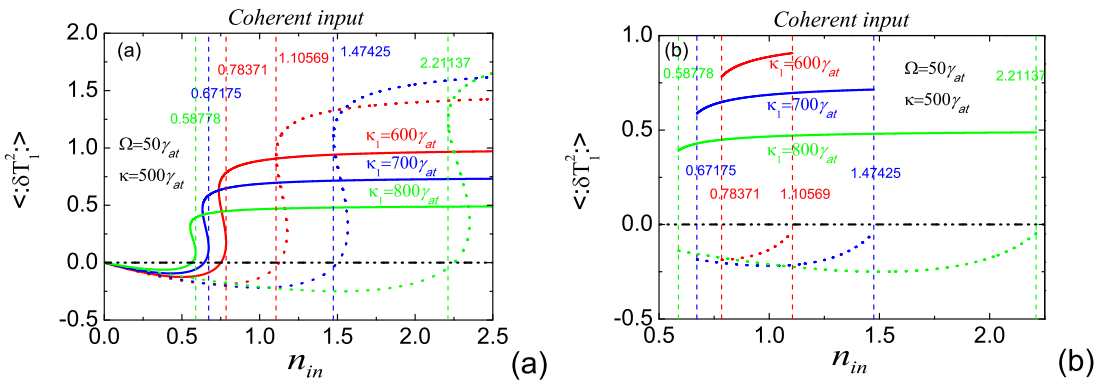

FIG. 5. The normally ordered variance $\langle{:}\,\delta T_1^2\,{:}\rangle$ for both forward and backward incidence as a function of input power $n_{\rm in}=|\alpha|^2$ with different cavity-loss rate κ_1: (a) the input power ranges from 0 to 2.5; (b) the input power falls into the optimal input window. All the solid and dotted curves represent the forward and backward incidence, respectively. The red, blue, and green vertical dashed curves correspond to the threshold values of each optimal window with $\kappa_1 = 600\gamma_{\rm at}$,$700\gamma_{\rm at}$, and $800\gamma_{\rm at}$, respectively. The common parameter is $\kappa = 500\gamma_{\rm at}$.

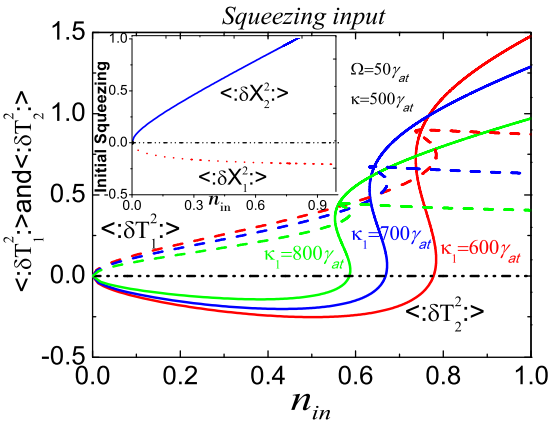

FIG. 6. The normally ordered variance $\langle : \delta T_1^2 : \rangle$ and $\langle : \delta T_2^2 : \rangle$ as a function of the input power $n_{\rm in}$ with different cavity-loss rates κ_1 for the forward incidence. All the solid and dashed curves represent $\langle : \delta T_2^2 : \rangle$ and $\langle : \delta T_1^2 : \rangle$ with $\kappa_1 = 600\gamma_{\rm at}, 700\gamma_{\rm at}$, and $800\gamma_{\rm at}$, respectively. The common parameter is $\kappa = 500\gamma_{\rm at}$.

$$\langle : \delta T_2^2 : \rangle = -\frac{\kappa_1\kappa_2[2\Omega^2 - \kappa\gamma_{\rm at}(1+x)](\cosh r \sinh r + \sinh^2 r)}{2\kappa^2[2\Omega^2+\kappa\gamma_{\rm at}(1+x)]} + \frac{\kappa_2\Omega^2 x}{4\kappa^2(1+x)}. \quad (27)$$

In the following, we restrict ourselves to the forward incidence and compare the squeezing of the transmitted light with that of the incident field. We plot $\langle : \delta T_1^2 : \rangle$ and $\langle : \delta T_2^2 : \rangle$ as a function of the input power $n_{\rm in} = \sinh^2 r$ with different cavity-loss rates κ_1 for the forward incidence in Fig. 6. The results show that the squeezing effect of the transmitted field can be observed when the input power is low (see the solid curves in Fig. 6), while as the input power falls into the optimal window, there is no squeezing of the output field which is similar to that for the coherent input case. However, from Fig. 6, we can find that the squeezing of the transmitted field is only exhibited in the phase quadrature, i.e., $\langle : \delta T_2^2 : \rangle < 0$, while there is no squeezing of the amplitude quadrature $\langle : \delta T_1^2 : \rangle \geqslant 0$ (see the dashed curves in Fig. 6) which is very different from the results obtained with a coherent light input. Furthermore, we note that the input light is an amplitude quadrature squeezed light $\langle : \delta X_1^2 : \rangle < 0$ (see the red dashed curve in the inset in Fig. 6), but there is only phase quadrature squeezing in the transmitted field, so the squeezing property of the amplitude quadrature has been transferred to the phase quadrature due to the coupling of the light and the atom. Moreover, compared with the coherent light input case, the degree of squeezing of the transmitted field with squeezed light input is much larger [i.e., see the blue solid curve in Figs. 5(a) and 6]. This means that the incident squeezed light improves the amount of squeezing of the transmitted field.

Finally, we discuss the change of squeezing between the transmitted field and the input squeezed light. The degree of squeezing can be expressed in unite of decibels, defined as $-10\log_{10}[\langle \delta T_i^2 \rangle / \langle \delta T_i^2 \rangle_{\rm vac}]$. Here $\langle \delta T_i^2 \rangle_{\rm vac}$ is the quadrature variance of the vacuum state and possesses the constant value of $\langle \delta T_i^2 \rangle_{\rm vac} = 1/4$. The variance of the transmitted field is defined by $\langle \delta T_i^2 \rangle = \langle : \delta T_i^2 : \rangle + 1/4$. The degrees of squeezing

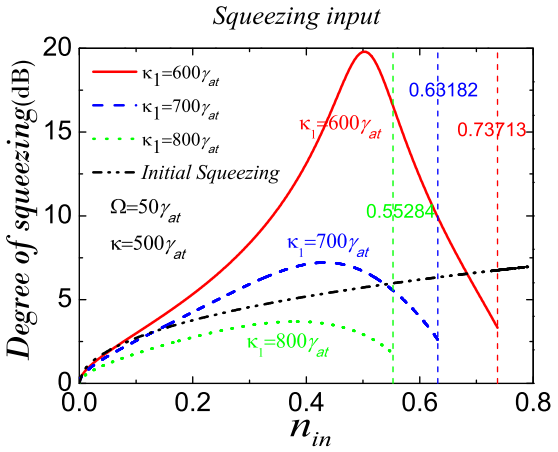

FIG. 7. The degree of the squeezing of the transmitted field and the initial input light as a function of the input power with different cavity-loss rates κ_1 for the forward incident. The red, blue, and green vertical dashed curves correspond to the threshold values of each optimal window with $\kappa_1 = 600\gamma_{\rm at}, 700\gamma_{\rm at}$, and $800\gamma_{\rm at}$, respectively. The common parameter is $\kappa = 500\gamma_{\rm at}$.

of the input lights and their transmitted field as a function of the input power $n_{\rm in}$ are shown in Fig. 7. It is clearly indicated that the degree of squeezing of the output field increases to its maximal at first, and then decrease with the increasing of the input power. In addition, the degree of the squeezing increases with the decreasing of the cavity-loss rate, and even becomes much larger than that of the initial input light when κ_1 decreases to a fixed value (see the red solid and blue dashed curves in Fig. 7). The reason is that, as the squeezed light is injected into the cavity, the input field and the cavity field gradually become correlated over time. This correlation is helpful for the coupling between the atom and cavity field, and then partial fluctuations in the input field can be canceled out, which leads to the enhancement of the squeezing of the output field [61].

From the above discussion, the squeezing effect of the output field strongly depends on the directions of the incident light. When the input power falls into the optimal window, the squeezing effect can only be observed for the backward case. Furthermore, the cavity-loss rate κ_1 has a profound influence on the squeezing of the transmitted field. Thus a high-degree squeezing state can be obtained by adjusting the asymmetry of the cavity.

V. CONCLUSION

In this paper, we investigate the quantum-statistical properties of the optical diode based on the cavity QED system with nonclassical light input. It turns out that an optical diode with high transmitted contrast and low operation power can be realized due to the separation of the bistable regimes. The optical diode is independent of the statistical properties of the input light but sensitive to the intensity. Our theoretical investigation implies a practical technique of realizing an optical diode by adjusting the cavity-loss rate and the intensity of the input light, which contributes to a variety of applications of quantum information processing. Furthermore, the quantum-statistical properties of the transmitted field have been discussed. Both the coherent and the squeezed

light inputs have been considered. The results show that the quantum-statistical properties of the transmitted field can be modified after propagating through the cavity QED system, and depend strongly on the cavity-loss rate, the direction, and the statistical properties of the input light. For the squeezed light input, the degree of squeezing of the transmitted field is much higher than that of the coherent light input. In addition, the interaction of the atom and the squeezed light enhances the amount of squeezing of the transmitted field and transfers the squeezing from the amplitude quadrature of the input light to the phase quadrature of the transmitted field.

ACKNOWLEDGMENTS

This work is partly supported by the National Natural Science Foundation of China (Grants No. 11574229, No. 1474221, and No. 11274242), the Joint Fund of the National Natural Science Foundation of China (Grant No. U1330203), the 973 program (Grant No. 2013CB632701), Shanghai Science and Technology Committee (Grant No. 15XD1503700), and the Shanghai Education Commission Foundation and Doctor Startup Fund of the Natural Science of Jinggangshan University (Grant No. JZB16003).

[1] G. S. Agarwal, Phys. Rev. Lett. **53**, 1732 (1984).
[2] A. Boca, R. Miller, K. M. Birnbaum, A. D. Boozer, J. McKeever, and H. J. Kimble, Phys. Rev. Lett. **93**, 233603 (2004).
[3] J. McKeever, A. Boca, A. D. Boozer, R. Miller, J. R. Buck, A. Kuzmich, and H. J. Kimble, Science **303**, 1992 (2004).
[4] J. K. Thompson, J. Simon, H.-Q. Loh, and V. Vuletic, Science **313**, 74 (2006).
[5] A. Auffèves-Garnier, C. Simon, J.-M.Gérard, and J.-P. Poizat, Phys. Rev. A **75**, 053823 (2007).
[6] I. Schuster, A. Kubanek, A. Fuhrmanek, T. Puppe, P. Pinkse, K. Murr, and G. Rempe, Nat. Phys. **4**, 382 (2008).
[7] R. J. Thompson, G. Rempe, and H. J. Kimble, Phys. Rev. Lett. **68**, 1132 (1992).
[8] P. W. H. Pinkse, T. Fischer, P. Maunz, and G. Rempe, Nature **404**, 365 (2000).
[9] A. Kuhn, M. Hennrich, and G. Rempe, Phys. Rev. Lett. **89**, 067901 (2002).
[10] T. Wilk, S. C. Webster, A. Kuhn, and G. Rempe, Science **317**, 488 (2007).
[11] Y. Colombe, T. Steinmetz, G. Dubois, F. Linke, D. Hunger, and J. Reichel, Nature **450**, 272 (2007).
[12] F. Brennecke, T. Donner, S. Ritter, T. Bourdel, M. Kohl, and T. Esslinger, Nature **450**, 268 (2007).
[13] W. L. Yang, Z. Q. Yin, Z. Y. Xu, M. Feng, and C. H. Oh, Phys. Rev. A **84**, 043849 (2011).
[14] G. M. A. Almeida, F. Ciccarello, T. J. G. Apollaro, and A. M. C. Souza, Phys. Rev. A **93**, 032310 (2016).
[15] G. S. Agarwal and Y. F. Zhu, Phys. Rev. A **92**, 023824 (2015).
[16] G. S. Agarwal, K. Di, L. Y. Wang, and Y. F. Zhu, Phys. Rev. A **93**, 063805 (2016).
[17] W. L. Chen, K. M. Beck, R. Buecker, M. Gullans, M. D. Lukin, H. Tanji-Suzuki, and V. Vuletic, Science **341**, 768 (2013).
[18] J. Volz and A. Rauschenbeutel, Science **341**, 725 (2013).
[19] A. Baas, J. P. Karr, H. Eleuch, and E. Giacobino, Phys. Rev. A **69**, 023809 (2004).
[20] T. Elsasser, B. Nagorny, and A. Hemmerich, Phys. Rev. A **69**, 033403 (2004).
[21] Y. Dumeige, A. M. Yacomotti, P. Grinberg, K. Bencheikh, E. LeCren, and J. A. Levenson, Phys. Rev. A **85**, 063824 (2012).
[22] S. Yang, M. Al-Amri, and M. S. Zubairy, Phys. Rev. A **87**, 033836 (2013).
[23] X. W. Xia, J. P. Xu, and Y. P. Yang, Phys. Rev. A **90**, 043857 (2014).
[24] X. W. Xia, J. P. Xu, and Y. P. Yang, J. Opt. Soc. Am. B **31**, 2175 (2014).
[25] A. B. Khanikaev and A. Alù, Nat. Photon. **9**, 359 (2015).
[26] Y. Shi, Z. F. Yu, and S. H. Fan, Nat. Photon. **9**, 388 (2015).
[27] D. Jalas, A. Petrov, M. Eich, W. Freude, S. Fan, Z. Yu, R. Baets, M. Popovic, A. Melloni, J. D. Joannopoulos, M. Vanwolleghem, C. R. Doerr, and H. Renner, Nat. Photon. **7**, 579 (2013).
[28] V. V. Konotop and V. Kuzmiak, Phys. Rev. B **66**, 235208 (2002).
[29] D.-W. Wang, H.-T. Zhou, M.-J. Guo, J.-X. Zhang, J. Evers, and S.-Y. Zhu, Phys. Rev. Lett. **110**, 093901 (2013).
[30] F. Fratini, E. Mascarenhas, L. Safari, J-Ph. Poizat, D. Valente, A. Auffèves, D. Gerace, and M. F. Santos, Phys. Rev. Lett. **113**, 243601 (2014).
[31] J. Dai, A. Roulet, H. N. Le, and V. Scarani, Phys. Rev. A **92**, 063848 (2015).
[32] S. V. Zhukovsky and A. G. Smirnov, Phys. Rev. A **83**, 023818 (2011).
[33] L. Feng, Y. L. Xu, W. S. Fegadolli, M. H. Lu, J. E. B. Oliveira, V. R. Almeida, Y. F. Chen, and A. Scherer, Nat. Mater. **12**, 108 (2013).
[34] H. Z. Shen, Y. H. Zhou, and X. X. Yi, Phys. Rev. A **90**, 023849 (2014).
[35] D. Roy, Phys. Rev. B **81**, 155117 (2010).
[36] Y. Shen, M. Bradford, and J. T. Shen, Phys. Rev. Lett. **107**, 173902 (2011).
[37] F. Fratini and R. Ghobadi, Phys. Rev. A **93**, 023818 (2016).
[38] M. J. Collett and R. Loudon, J. Opt. Soc. Am. B **4**, 1525 (1987).
[39] E. A. Sete and H. Eleuch, Phys. Rev. A **82**, 043810 (2010).
[40] P. Schwendimann and A. Quattropani, Phys. Rev. A **86**, 043811 (2012).
[41] A. Grankin, E. Brion, E. Bimbard, R. Boddeda, I. U. Usmani, A. Ourjoumtsev, and P. Grangier, New J. Phys. **16**, 043020 (2014).
[42] H. J. Carmichael, Phys. Rev. Lett. **55**, 2790 (1985).
[43] J. J. Mendoza-Arenas, S. R. Clark, S. Felicetti, G. Romero, E. Solano, D. G. Angelakis, and D. Jaksch, Phys. Rev. A **93**, 023821 (2016).
[44] C. H. Huang, Y. H. Wen, and Y.W. Liu, Opt. Express **24**, 4278 (2016).
[45] J. F. Huang, J. Q. Liao, and C. P. Sun, Phys. Rev. A **87**, 023822 (2013).
[46] Q. A. Turchette, N. P. Georgiades, C. J. Hood, H. J. Kimble, and A. S. Parkins, Phys. Rev. A **58**, 4056 (1998).
[47] B. Yurke, Phys. Rev. A **29**, 408 (1984).
[48] B. Yurke, Phys. Rev. A **32**, 300 (1985).
[49] M. J. Collett and D. F. Walls, Phys. Rev. A **32**, 2887 (1985).
[50] D. M. Hope, H. A. Bachor, P. J. Manson, D. E. McClelland, and P. T. H. Fisk, Phys. Rev. A **46**, R1181 (1992).

[51] M. Fernee, P. Kinsler, and P. D. Drummond, Phys. Rev. A **51**, 864 (1995).
[52] C. Navarrete-Benlloch, A. Romanelli, E. Roldán, and G. J. de Valćarcel, Phys. Rev. A **81**, 043829 (2010).
[53] H. H. Adamyan, J. A. Bergou, N. T. Gevorgyan, and G. Y. Kryuchkyan, Phys. Rev. A **92**, 053818 (2015).
[54] E. A. Sete, H. Eleuch, and S. Das, Phys. Rev. A **84**, 053817 (2011).
[55] T. P. Purdy, P.-L. Yu, R.W. Peterson, N. S. Kampel, and C. A. Regal, Phys. Rev. X **3**, 031012 (2013).
[56] K. Qu and G. S. Agarwal, Phys. Rev. A **91**, 063815 (2015).
[57] G. S. Agarwal and S. M. Huang, Phys. Rev. A **93**, 043844 (2016).
[58] A. K. Chauhan and A. Biswas, Phys. Rev. A **94**, 023831 (2016).
[59] C. W. Gardiner and M. J. Collett, Phys. Rev. A **31**, 3761 (1985).
[60] M. J. Collett and C. W. Gardiner, Phys. Rev. A **30**, 1386 (1984).
[61] M. O. Scully and M. S. Zubairy, *Quantum Optics* (Cambridge University Press, Cambridge, 1997).